

Published in final edited form as:

*Astron Astrophys.* 2016 December ; 596: . doi:10.1051/0004-6361/201629913.

## Trans-cis molecular photoswitching in interstellar Space\*

S. Cuadrado<sup>1</sup>, J. R. Goicoechea<sup>1</sup>, O. Roncero<sup>2</sup>, A. Aguado<sup>3</sup>, B. Tercero<sup>1</sup>, and J. Cernicharo<sup>1</sup>

<sup>1</sup>Grupo de Astrofísica Molecular. Instituto de Ciencia de Materiales de Madrid (ICMM-CSIC), Sor Juana Ines de la Cruz 3, E-28049 Cantoblanco, Madrid, Spain

<sup>2</sup>Instituto de Física Fundamental (IFF-CSIC). Calle Serrano 123, E-28006 Madrid, Spain

<sup>3</sup>Facultad de Ciencias, Unidad Asociada de Química-Física Aplicada CSIC-UAM, Universidad Autónoma de Madrid, E-28049, Madrid, Spain

### Abstract

As many organic molecules, formic acid (HCOOH) has two conformers (*trans* and *cis*). The energy barrier to internal conversion from *trans* to *cis* is much higher than the thermal energy available in molecular clouds. Thus, only the most stable conformer (*trans*) is expected to exist in detectable amounts. We report the first interstellar detection of *cis*-HCOOH. Its presence in ultraviolet (UV) irradiated gas exclusively (the Orion Bar photodissociation region), with a low *trans*-to-*cis* abundance ratio of  $2.8 \pm 1.0$ , supports a photoswitching mechanism: a given conformer absorbs a stellar photon that radiatively excites the molecule to electronic states above the interconversion barrier. Subsequent fluorescent decay leaves the molecule in a different conformer form. This mechanism, which we specifically study with *ab initio* quantum calculations, was not considered in Space before but likely induces structural changes of a variety of interstellar molecules submitted to UV radiation.

### Keywords

Astrochemistry; Line: identification; ISM: clouds; ISM: molecules; Photon-dominated region (PDR)

## 1 Introduction

Conformational isomerism refers to isomers (molecules with the same formula but different chemical structure) having the same chemical bonds but different geometrical orientations around a single bond. Such isomers are called conformers. An energy barrier often limits the isomerization. This barrier can be overcome by light. Photoisomerization (or photoswitching) has been studied in ice IR-irradiation experiments (e.g. Maçôas et al. 2004), in biological processes, and, for large polyatomic molecules, also in gas-phase experiments (Ryan & Levy 2001). HCOOH is the simplest organic acid and has two conformers (*trans* and *cis*) depending on the orientation of the hydrogen single bond. The most stable *trans*

s.cuadrado@icmm.csic.es; jr.goicoechea@icmm.csic.es, jose.cernicharo@csic.es.

\*This paper makes use of observations obtained with the IRAM-30 m telescope. IRAM is supported by INSU/CNRS (France), MPG (Germany), and IGN (Spain).

conformer was the first acid detected in the interstellar medium, ISM (Zuckerman et al. 1971). Gas-phase *trans*-HCOOH shows moderate abundances towards hot cores (Liu et al. 2001) and hot corinos (Cazaux et al. 2003), in cold dark clouds (Cernicharo et al. 2012), and in cometary coma (Bockelée-Morvan et al. 2000). Solid HCOOH is present in interstellar ices (Keane et al. 2001) and in chondritic meteorites (Briscoe & Moore 1993).

The ground-vibrational state of *cis*-HCOOH is  $1365 \pm 30 \text{ cm}^{-1}$  higher in energy than the *trans* conformer (Hocking 1976). The energy barrier to internal rotation (the conversion from *trans* to *cis*) is about  $4827 \text{ cm}^{-1}$  (Hocking 1976), approximately 7000 K in temperature units. This is much higher than the thermal energy available in molecular clouds (having typical temperatures from about 10 to 300 K). Generalizing this reasoning, only the most stable conformer of a given species would be expected in such clouds. Photoswitching, however, may be a viable mechanism producing the less stable conformers in detectable amounts: a given conformer absorbs a high-energy photon that radiatively excites the molecule to electronic states above the interconversion energy barrier. Subsequent radiative decay to the ground-state would leave the molecule in a different conformer.

In this work we have searched for pure rotational lines of the *trans*- and *cis*-HCOOH conformers in the 3 millimetre spectral band. We observed three prototypical interstellar sources known to display a very rich chemistry and bright molecular line emission: (i) the Orion Bar photodissociation region (PDR): the edge of the Orion cloud irradiated by ultraviolet (UV) photons from nearby massive stars (e.g. Goicoechea et al. 2016), (ii) the Orion hot core: warm gas around massive protostars (e.g. Tercero et al. 2010), and (iii) Barnard 1-b (B1-b): a cold dark cloud (e.g. Cernicharo et al. 2012). The two latter sources are shielded from strong UV radiation fields. We only detect *cis*-HCOOH towards the Orion Bar. This represents the first interstellar detection of the conformer.

## 2 Source selection and observations

Because of its nearly edge-on orientation, the Orion Bar PDR is a template source to study the molecular content as the far-UV radiation field (FUV; stellar photons with energies below 13.6 eV, or wavelengths ( $\lambda$ ) longer than  $911 \text{ \AA}$ , the hydrogen atom ionisation threshold) is attenuated from the cloud edge to the interior (Hollenbach & Tielens 1999). The impinging FUV radiation field at the edge of the Bar is about  $4 \times 10^4$  times the mean interstellar radiation field (e.g. Goicoechea et al. 2016, and references therein). We observed three positions of the Bar characterized by a decreasing FUV photon flux.

We have used the IRAM-30 m telescope (Pico Veleta, Spain) and the 90 GHz EMIR receiver. We employed the Fast Fourier Transform Spectrometer (FFTS) backend at 200 kHz spectral resolution ( $0.7 \text{ km s}^{-1}$  at 90 GHz). Observations towards the Orion Bar are part of a complete millimetre (mm) line survey (80 – 360 GHz, Cuadrado et al. 2015). They include specific deep searches for HCOOH lines in the 3 mm band towards three different positions located at a distance of  $14''$ ,  $40''$ , and  $65''$  from the ionisation front (Fig. 1A). Their offset coordinates with respect to the  $\alpha_{2000} = 05^{\text{h}} 35^{\text{m}} 20.1^{\text{s}}$ ,  $\delta_{2000} = -05^{\circ} 25' 07.0''$  position at the ionisation front are  $(+10'', -10'')$ ,  $(+30'', -30'')$ , and  $(+35'', -55'')$ . The observing procedure was position switching with a reference position at  $(-600'', 0'')$  to avoid the

extended emission from the Orion molecular cloud. The half power beam width (HPBW) at 3 mm ranges from  $\sim 30.8''$  to  $21.0''$ . We reduced and analysed the data using the GILDAS software as described in Cuadrado et al. (2015). The antenna temperature,  $T_A^*$ , was converted to the main beam temperature,  $T_{MB}$ , using  $T_{MB} = T_A^* / \eta_{MB}$ , where  $\eta_{MB}$  is the antenna efficiency ( $\eta_{MB} = 0.87 - 0.82$  at 3 mm). The rms noise obtained after 5 h integration is  $\sim 1 - 5$  mK per resolution channel.

We also searched for HCOOH in regions shielded from strong FUV radiation fields (see Appendix E). We selected two chemically rich sources for which we have also carried out deep mm-line surveys with the IRAM-30m telescope: towards the hot core in Orion BN/KL (Tercero et al. 2010) and towards the quiescent dark cloud Barnard 1-b (B1-b; Cernicharo et al. 2012).

### 3 Results

#### 3.1 Line identification

We specifically computed the *cis*-HCOOH rotational lines frequencies by fitting the available laboratory data (Winnewisser et al. 2002) with our own spectroscopic code, MADEX (Cernicharo 2012). The standard deviation of the fit is 60 kHz. For the *trans* conformer, higher frequency laboratory data (Cazzoli et al. 2010) were also used in a separate fit. The standard deviation of the fit for *trans*-HCOOH is 42 kHz. These deviations are smaller than the frequency resolution of the spectrometer we used to carry out the astronomical observations. Formic acid is a near prolate symmetric molecule with rotational levels distributed in different  $K_a$  rotational ladders ( $K_a = 0, 1, 2, \dots$ ). Both *a*- and *b*-components of its electric dipole moment  $\mu$  exist (Winnewisser et al. 2002). The dipole moments of the *cis* conformer ( $\mu_a = 2.650$  D and  $\mu_b = 2.710$  D, Hocking 1976) are stronger than those of the *trans* conformer ( $\mu_a = 1.421$  D and  $\mu_b = 0.210$  D, Kuze et al. 1982).

In total, we identify 12 rotational lines of *cis*-HCOOH and 10 of *trans*-HCOOH above  $3\sigma$  towards the FUV-illuminated edge of the Orion Bar, ( $+10''$ ,  $-10''$ ) position. The detected lines from the *cis*- and *trans*-HCOOH are shown in Figs. 2 and D.1, respectively. Lines attributed to HCOOH show a Gaussian line profile centred at the systemic velocity of the Orion Bar ( $10.4 \pm 0.3$  km s $^{-1}$ ). Lines are narrow, with linewidths of  $1.9 \pm 0.3$  km s $^{-1}$ . The large number of detected lines, and the fact that none of the lines correspond to transitions of abundant molecules known to be present in the Bar or in spectroscopic line catalogues, represents a robust detection of the *cis* conformer. The observational parameters and Gaussian fit results are tabulated in Tables F.1 and F.2 for the *cis* and *trans* conformer, respectively.

#### 3.2 Line stacking analysis

Complex organic molecules have relatively low abundances in FUV-irradiated interstellar gas (Guzmán et al. 2014). Indeed, detected *trans*-HCOOH lines are faint. To improve the statistical significance of our search towards the positions inside the Bar, we performed a “line stacking” analysis. For each observed position, we added spectra at the expected frequency of several HCOOH lines that could be present within the noise level (sharing

similar rotational level energies and Einstein coefficients). The spectra in frequency scale were first converted to local standard of rest (LSR) velocity scale and resampled to the same velocity channel resolution before stacking. We repeated this procedure for *trans*-HCOOH lines. This method allows us to search for any weak line signal from the two conformers that could not be detected individually.

Figure 1B shows a comparison of the stacking results for *cis* and *trans*-HCOOH lines towards the three target positions in the Bar. Although we detect *trans*-HCOOH in all positions, emission from the *cis* conformer is only detected towards the position located closer to the cloud edge, (+10", -10"). They demonstrate that *cis*-HCOOH is detected close the FUV-illuminated edge of the Bar, but the emission disappears towards the more shielded cloud interior.

A similar stacking analysis was carried out for the Orion hot core and B1-b spectra. Although we detect several *trans*-HCOOH lines, the *cis* conformer was not detected towards the hot core and the cold dark cloud (see Appendix E).

### 3.3 Trans-to-cis abundance ratios

Given the number of HCOOH lines detected towards the Bar, we can determine the column density and rotational temperatures of both conformers accurately (see Appendix D). In particular, we infer a low *trans*-to-*cis* abundance ratio of  $2.8 \pm 1.0$ . The nondetection of *cis*-HCOOH towards the Orion hot core and B1-b (see Appendix E) provides much higher *trans*-to-*cis* limits ( $>100$  and  $>60$ , respectively). This suggests that the presence of *cis*-HCOOH in the Orion Bar PDR is related to the strong FUV field permeating the region.

## 4 Photoisomerization rates and discussion

Photolysis of HCOOH has been widely studied, both experimentally (Sugarman 1943; Ioannoni et al. 1990; Brouard & Wang 1992; Su et al. 2000) and theoretically (Beaty-Travis et al. 2002; He & Fang 2003; Maeda et al. 2015). Dissociation of HCOOH takes place after absorption of FUV photons with energies greater than  $\sim 5$  eV ( $\lambda < 2500$  Å). Recently, Maeda et al. (2015) determined that this dissociation threshold coincides with the crossing of the  $S_0$  and  $T_1$  electronic states of the molecule. The specific products of the photofragmentation process (of the different photodissociation channels) depend on the specific energy of the FUV photons and on the initial HCOOH conformer. Interestingly, absorption of lower energy photons does not dissociate the molecule but induces fluorescent emission. In particular, HCOOH fluorescence from the  $S_1$  excited electronic state has been observed in laser-induced experiments performed in the  $\lambda = 2500 - 2700$  Å range (Ioannoni et al. 1990; Brouard & Wang 1992). These studies indicate that the geometrical configuration of the two hydrogen atoms is different in the  $S_0$  and  $S_1$  states. The fluorescence mechanism from the  $S_1$  state is a likely route for the *trans*  $\rightarrow$  *cis* isomerization. In addition, the isomerization barrier from the  $S_1$  state ( $\sim 1400$  cm $^{-1}$ ) is much lower than from the ground.

In order to quantify the role of the photoswitching mechanism, we carried out *ab initio* quantum calculations and determined the HCOOH potential energy surfaces of the  $S_0$  and  $S_1$

electronic states as a function of the two most relevant degrees of freedom,  $\phi_1$  the torsional angle of OH and  $\phi_2$ , the torsional angle of CH (see Appendix A and Fig. A.1). With this calculation we can compute the position of the photon absorptions leading to fluorescence (those in the approximate  $\lambda = 2300 - 2800 \text{ \AA}$  range), and the probabilities to fluoresce from one conformer to the other (the *trans-to-cis* and *cis-to-trans* photoswitching cross-sections and probabilities, see Fig. 3).

With a knowledge of  $N_{\text{ph}}(\lambda)$ , the FUV photon flux in units of  $\text{photon cm}^{-2} \text{ s}^{-1} \text{ \AA}^{-1}$ , we can calculate the number of *trans-to-cis* and *cis-to-trans* photoisomerizations per second ( $\xi_{\text{tc}}$  and  $\xi_{\text{ct}}$ , respectively. See Appendix B). In the absence of any other mechanism destroying HCOOH, the  $\xi_{\text{ct}}/\xi_{\text{tc}}$  ratio provides the *trans-to-cis* abundance ratio in equilibrium. The time needed to reach the equilibrium ratio is then  $(\xi_{\text{tc}} + \xi_{\text{ct}})^{-1} \cdot N_{\text{ph}}(\lambda)$ , and thus  $\xi_{\text{tc}}$  and  $\xi_{\text{ct}}$  depend on the FUV radiation sources (type of star) and on the cloud position. Describing the cloud depth position in terms of the visual extinction into the cloud ( $A_V$ ), one magnitude of extinction is equivalent to a column density of about  $10^{21} \text{ H}_2$  molecules per  $\text{cm}^{-2}$  in the line-of-sight.

In general (for a flat, wavelength-independent FUV radiation field), HCOOH photodissociation will always dominate over fluorescence (photodissociation cross-sections are larger and the relevant photons can be absorbed over a broader energy range,  $E > 5 \text{ eV}$ ). The strength and shape of the interstellar FUV radiation field, however, is a strong function of  $A_V$  and is very sensitive to the dust and gas absorption properties. Because of the wavelength-dependence of the FUV-absorption process,  $N_{\text{ph}}(\lambda)$  drastically changes as one moves from the cloud edge to the shielded interior. In particular, the number of low-energy FUV photons (e.g. below 5 eV) relative to the high-energy photons (e.g. those above 11 eV dissociating molecules such as CO and ionising atoms such as carbon) increases with  $A_V$ . In this work we used a FUV radiative transfer and thermo-chemical model (Le Petit et al. 2006; Goicoechea & Le Boulrot 2007) to estimate  $N_{\text{ph}}(\lambda)$  at different positions of the Orion Bar. The well-known “2175 Å bump” of the dust extinction curve (absorption of  $\lambda = 1700 - 2500 \text{ \AA}$  photons by PAHs and small carbonaceous grains, Cardelli et al. 1989; Joblin et al. 1992) greatly reduces the number of HCOOH dissociating photons relative to those producing HCOOH fluorescence (Fig. 3, bottom panel). The resulting FUV radiation spectrum,  $N_{\text{ph}}(\lambda)$ , at different  $A_V$  is used to calculate  $\xi_{\text{tc}}$  and  $\xi_{\text{ct}}$  (Table B.1). We determine that at a cloud depth of about  $A_V = 2 - 3 \text{ mag}$ , and if the number of HCOOH dissociating photons is small compared to the number of photons producing photoisomerization (i.e. most photons with  $E > 5 \text{ eV}$  have been absorbed), the *cis* conformer should be detectable with a *trans-to-cis* abundance ratio of about 3.5 – 4.1. These values are remarkably close to the *trans-to-cis* ratio inferred from our observations of the Bar.

Closer to the irradiated cloud edge ( $A_V = 0 - 2 \text{ mag}$ ), photodissociation destroys the molecule much faster than the time needed for the *trans-to-cis* isomerization. On the other hand, too deep inside the cloud, the flux of  $E > 5 \text{ eV}$  photons decreases to values for which the isomerization equilibrium would take an unrealistic amount of time ( $>10^6$  years for  $A_V = 5 \text{ mag}$ ). Therefore, our detection of *cis*-HCOOH in irradiated cloud layers where CO becomes the dominant carbon carrier (a signature of decreasing flux of high-energy FUV photons) agrees with the photoswitching scenario.

For standard grain properties and neglecting HCOOH photodissociation, we calculate that the time needed to achieve a low *trans-to-cis* abundance ratio and make *cis*-HCOOH detectable at  $A_V = 2 - 3$  mag is  $10^4 - 10^5$  years (see Table B.1). This is reasonably fast, and shorter than the cloud lifetime. In practice, it is not straightforward to quantify the exact contribution of HCOOH photodissociation and photoisomerization at different cloud positions. The above time-scales require that the flux of  $E > 5$  eV dissociating photons is small compared to those producing fluorescence. This depends on the specific dust absorption properties, that sharply change with  $A_V$  as dust populations evolve (Draine 2003), on the strength and width of the 2175 Å extinction bump, and on the role of molecular electronic transitions blanketing the FUV spectrum. The similar *trans*-HCOOH line intensities observed towards the three positions of the Bar (Fig. 1) suggest that even if the HCOOH photodestruction rate increases at the irradiated cloud edge, the HCOOH formation rate (from gas-phase reactions or desorbing directly from grain surfaces, Garrod et al. 2008) must increase as well. The inferred HCOOH abundances are not particularly high,  $(0.6 - 3.0) \times 10^{-10}$  with respect to H. Hence, modest HCOOH photodestruction and formation rates are compatible with the photoswitching mechanism occurring in realistic times.

Although the observed abundances of *trans*- and *cis*-HCOOH in the Orion Bar are compatible with gas-phase photoisomerization, we note that photoswitching may also occur on the surface of grains covered by HCOOH ices. In a similar way, solid HCOOH (mostly *trans*) can absorb FUV photons that switch the molecule to the *cis* form before being desorbed. Once in the gas, both conformers will continue their photoisomerization following absorption of  $\lambda \gtrsim 2500$  Å photons. Laboratory experiments are needed to quantify the mechanisms leading to HCOOH ice photoswitching by FUV photon absorption.

Searching for further support to the FUV photoswitching scenario, we qualitatively explored two other possibilities for the *trans-to-cis* conversion. First, the isomerization of solid HCOOH after IR irradiation of icy grain surfaces (as observed in the laboratory, Maçôas et al. 2004; Olbert-Majkut et al. 2008) and subsequent desorption to the gas-phase. Second, the gas-phase isomerization by collisions of HCOOH with energetic electrons ( $\sim 0.5$  eV). We concluded that if these were the dominant isomerization mechanisms, emission lines from *cis*-HCOOH would have been detected in other interstellar sources (see Appendix C).

Isomerization by absorption of UV photons was not considered as a possible mechanism to induce structural changes of molecules in interstellar gas. The detection of *cis*-HCOOH towards the Orion Bar opens new avenues to detect a variety of less stable conformers in Space. This can have broad implications in astrochemistry and astrobiology.

## Supplementary Material

Refer to Web version on PubMed Central for supplementary material.

## Acknowledgements

We thank N. Marcelino for helping with the observations of B1-b. We thank the ERC for support under grant ERC-2013-Syg-610256-NANOCOSMOS. We also thank Spanish MINECO for funding support under grants

AYA2012-32032 and FIS2014-52172-C2, and from the CONSOLIDER-Ingenio program “ASTROMOL” CSD 2009-00038. IRAM is supported by INSU/CNRS (France), MPG (Germany), and IGN (Spain).

## References

- Beaty-Travis LM, Moule DC, Lim EC, Judge RH. *J Chem Phys.* 2002; 117:4831.
- Blake GA, Sutton EC, Masson CR, Phillips TG. *ApJ.* 1987; 315:621.
- Bockelée-Morvan D, Lis DC, Wink JE, et al. *A&A.* 2000; 353:1101.
- Briscoe JF, Moore CB. *Meteoritics.* 1993; 28:330.
- Brouard M, Wang J-X. *J Chem Soc Faraday Trans.* 1992; 88:3511.
- Cardelli JA, Clayton GC, Mathis JS. *ApJ.* 1989; 345:245.
- Cazaux S, Tielens AGGM, Ceccarelli C, et al. *ApJ.* 2003; 593:L51.
- Cazzoli G, Puzzarini C, Stopkowicz S, Gauss J. *A&A.* 2010; 520:A64.
- Cernicharo, J. Vol. 58. *EAS Publications Series*; 2012. p. 251-26.
- Cernicharo J, Kisiel Z, Tercero B, et al. *A&A.* 2016; 587:L4.
- Cernicharo J, Marcelino N, Roueff E, et al. *ApJ.* 2012; 759:L43.
- Cuadrado S, Goicoechea JR, Pilleri P, et al. *A&A.* 2015; 575:A82.
- Draine BT. *ApJS.* 1978; 36:595.
- Draine BT. *ARA&A.* 2003; 41:241.
- Garrod RT, Widicus Weaver SL, Herbst E. *ApJ.* 2008; 682:283.
- Gerin M, Pety J, Fuente A, et al. *A&A.* 2015; 577:L2.
- Goicoechea JR, Le Bourlot J. *A&A.* 2007; 467:1.
- Goicoechea JR, Pety J, Cuadrado S, et al. *Nature.* 2016; 537:207. [PubMed: 27509859]
- Goldsmith PF, Langer WD. *ApJ.* 1999; 517:209.
- Guzmán VV, Pety J, Gratier P, et al. *Faraday Discussions.* 2014; 168:103. [PubMed: 25302376]
- He H-Y, Fang W-H. *Journal of the American Chemical Society.* 2003; 125:16139. [PubMed: 14678006]
- Hocking WH. *Zeitschrift Naturforschung Teil A.* 1976; 31:1113.
- Hollenbach DJ, Tielens AGGM. *Reviews of Modern Physics.* 1999; 71:173.
- Ioannoni F, Moule DC, Clouthier DJ. *The Journal of Physical Chemistry.* 1990; 94:2290.
- Joblin C, Leger A, Martin P. *ApJ.* 1992; 393:L79.
- Jørgensen JK, Harvey PM, Evans NJ II, et al. *ApJ.* 2006; 645:1246.
- Keane JV, Tielens AGGM, Boogert ACA, Schutte WA, Whittet DCB. *A&A.* 2001; 376:254.
- Kuze H, Kuga T, Shimizu T. *Journal of Molecular Spectroscopy.* 1982; 93:248.
- Le Petit F, Nehmé C, Le Bourlot J, Roueff E. *ApJS.* 2006; 164:506.
- Li A, Draine BT. *ApJ.* 2001; 554:778.
- Liu S-Y, Mehringer DM, Snyder LE. *ApJ.* 2001; 552:654.
- Maçôas EMS, Khriachtchev L, Pettersson M, Fausto R, Räsänen M. *J Chem Phys.* 2004; 121:1331. [PubMed: 15260676]
- Maeda S, Taketsugu T, Morokuma K. *The Journal of Physical Chemistry Letters.* 2012; 3:1900. [PubMed: 26292011]
- Maeda S, Taketsugu T, Ohno K, Morokuma K. *Journal of the American Chemical Society.* 2015; 137:3433.
- Marcelino, N. Universidad de Granada, Spain: 2007. PhD thesis
- Öberg KI, Bottinelli S, Jørgensen JK, van Dishoeck EF. *ApJ.* 2010; 716:825.
- Olbert-Majkut A, Ahokas J, Lundell J, Pettersson M. *J Chem Phys.* 2008; 129:041101. [PubMed: 18681623]
- Ryan WL, Levy DH. *Journal of the American Chemical Society.* 2001; 123:961. [PubMed: 11456631]
- Su H, He Y, Kong F, Fang W, Liu R. *J Chem Phys.* 2000; 113:1891.
- Sugarman B. *Proceedings of the Physical Society.* 1943; 55:429.

- Tercero B, Cernicharo J, Pardo JR, Goicoechea JR. *A&A*. 2010; 517:A96.
- van Dishoeck EF, Black JH. *ApJ*. 1982; 258:533.
- Walmsley CM, Natta A, Oliva E, Testi L. *A&A*. 2000; 364:301.
- Werner H-J, Knowles PJ, Knizia G, Manby FR, Schtz M. *Wiley Interdisciplinary Reviews: Computational Molecular Science*. 2012; 2:242.
- Winnewisser M, Winnewisser BP, Stein M, et al. *Journal of Molecular Spectroscopy*. 2002; 216:259.
- Zuckerman B, Ball JA, Gottlieb CA. *ApJ*. 1971; 163:L41.



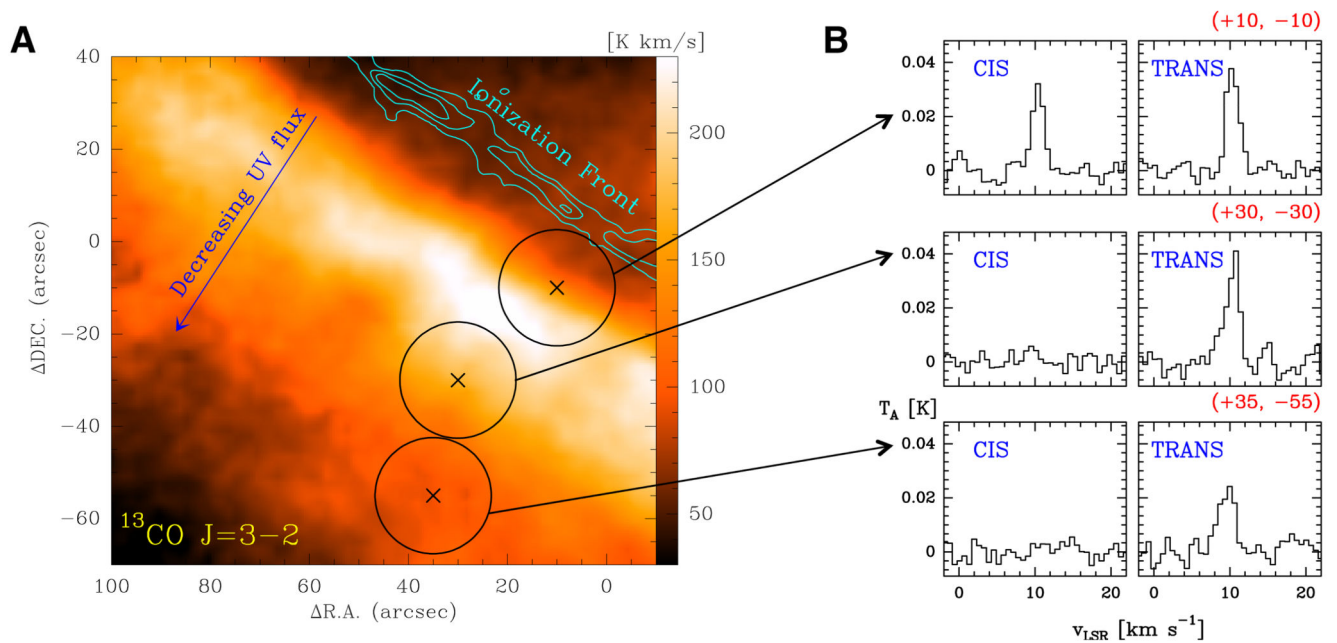


**Fig. 1.**

Detection of *cis*-HCOOH towards the FUV-illuminated edge of the Orion Bar. *Left:*  $^{13}\text{CO } J=3 \rightarrow 2$  integrated emission image with a HPBW of  $8'$  obtained with the IRAM-30 m telescope (Cuadrado et al. in prep.). The cyan contour marks the position of neutral cloud boundary traced by the  $\text{O I } 1.317 \mu\text{m}$  fluorescent line emission (in contours from 3 to 7 by  $2 \times 10^{-4} \text{ erg s}^{-1} \text{ cm}^{-2} \text{ sr}^{-1}$ ; Walmsley et al. 2000). *Right:* *Cis*- and *trans*-HCOOH stacked spectra towards the observed positions.

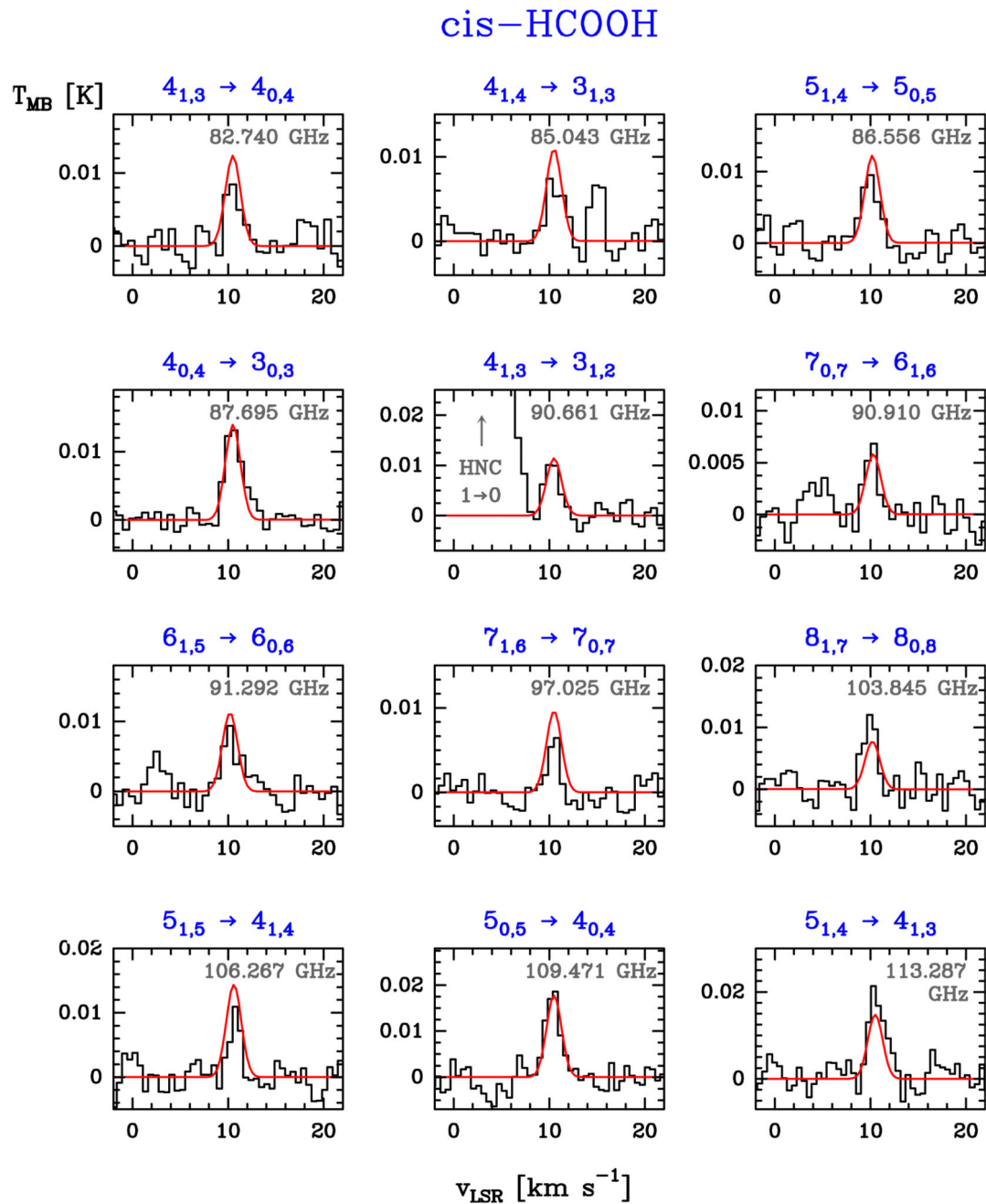


**Fig. 2.** Detected *cis*-HCOOH rotational lines towards the Orion Bar, (+10'', -10'') position. The ordinate refers to the intensity scale in main beam temperature units, and the abscissa to the LSR velocity. Line frequencies (in GHz) are indicated at the top-right of each panel together with the rotational quantum numbers (in blue). The red curve shows an excitation model that reproduces the observations.

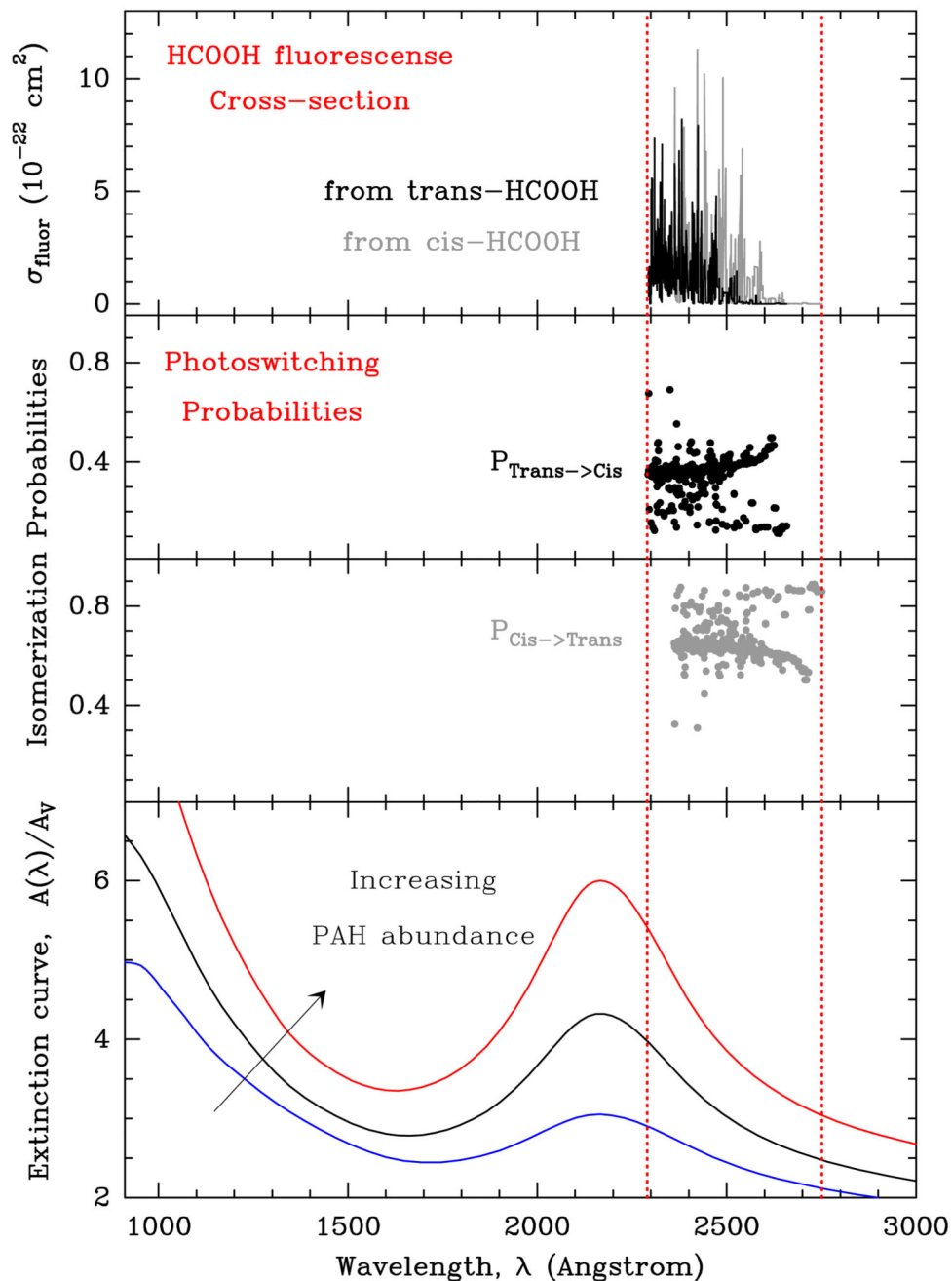


**Fig. 3.** *Ab initio* absorption cross-sections and photoisomerization probabilities computed in this work. *Top panel:* *trans*- and *cis*-HCOOH absorption cross-sections for photons with  $E < 5$  eV (those leading to fluorescence). *Middle panels:* normalized probabilities of bound-bound decays producing isomerization (*trans*  $\rightarrow$  *cis* and *cis*  $\rightarrow$  *trans*). *Bottom panel:* standard interstellar dust extinction curve (blue). Black and red curves show the effect of an increased PAH abundance.